Article

Not peer-reviewed version

One-Step Synthesis, Crystallography, and Acute Toxicity of Two Boronic-Carbohydrate Adducts which Induced Sedation in Mice

Ricardo Iván Córdova-Chávez , José G. Trujillo-Ferrara * , Itzia I. Padilla-Martínez , Hector Gonzalez-Espinosa , Antonio Abad-García , Eunice D. Farfán-García , Clara Ortega-Camarillo , Alejandra Contreras-Ramos , Marvin A. Soriano-Ursua *

Posted Date: 21 May 2024

doi: 10.20944/preprints202405.1343.v1

Keywords: Boron; Carbohydrate; Sedation; Acute toxicity; Adducts; neurons; mice.

 doi:10.20944/preprints202405.1343.v1

Article

One-Step Synthesis, Crystallography, and Acute Toxicity of Two Boronic-Carbohydrate Adducts which Induced Sedation in Mice

Ricardo Ivan Cordova-Chávez [1,2], José G. Trujillo-Ferrara [2,*], Itzia I. Padilla-Martínez [3], Héctor González-Espinosa [1], Antonio Abad-García [1], Eunice D. Farfán-García [2], Clara Ortega-Camarillo [4], Alejandra Contreras-Ramos [5] and Marvin A. Soriano-Ursúa [1,*]

[1] Laboratorio de Neurofisiología, Sección de Estudios de Posgrado e Investigación, Escuela Superior de Medicina, Instituto Politécnico Nacional. Plan de San Luis y Díaz Mirón s/n 11340, Mexico City, Mexico. R.I.C-C ivancoch@hotmail.com; H.G-E. gonzalezespinosahector@gmail.com; A.A-G. abadantonio19315@gmail.com; M.A.S-U. msoriano@ipn.mx

[2] Laboratorio de bioquímica, Sección de Estudios de Posgrado e Investigación, Escuela Superior de Medicina, Instituto Politécnico Nacional. Plan de San Luis y Díaz Mirón s/n 11340, Mexico City, Mexico J.G.T-F. jtrujillo@ipn.mx; E.D.F-G. efarfang@ipn.mx

[3] Laboratorio de Química Supramolecular y Nanociencias, Unidad Profesional Interdisciplinaria de Biotecnología, Instituto Politécnico Nacional, Mexico city, Mexico. I.I.P-M. ipadillamar@ipn.mx

[4] Medical Research Unit in Biochemistry, Specialties Hospital, National Medical Center SXXI, Instituto Mexicano del Seguro Social, Av. Cuauhtémoc 330, Col. Doctores, Del. Cuauhtémoc CP, 06720 CDMX, Mexico. C.O-C. cocamarillo2014@gmail.com

[5] Laboratory of Molecular Biology in the Congenital Malformations Unit. Children's Hospital of Mexico Federico Gomez (HIMFG), Mexico City, Mexico. A.C-R. acora_ramos@hotmail.com

* Correspondence: M.A.S-U. msoriano@ipn.mx; Phone: (+52 57296000 - 62751). J.G.T-F. jtrujillo@ipn.mx; Phone: (+52 57296000 - 62747).

Abstract: Background: Boronic acids form di-ester bonds with cis-hydroxyl groups in carbohydrates. The formation of these adducts could impair the physical and chemical properties of the precursors, even their biological activity. **Methods:** Two carbohydrate-derivatives from D-fructose and D-arabinose and phenylboronic acid were synthesized in a straightforward one-step procedure and chemically characterized by spectroscopy and X-ray diffraction crystallography. Also, an acute toxicity test was performed to determine their Lethal Dose$_{50}$ (LD$_{50}$) by using the Lorke's method. **Results:** Analytical chemistry assays confirmed adducts by the generation of the diester bonds with a β-D-pyranose of carbohydrates, including signals corresponding to the formation of new bonds, like the stretching of B-O bonds. The NMR spectra yielded information about the stereoselectivity in the synthesis reaction by the finding of just one signal in the range for the anomeric carbon in the ^{13}C NMR spectra of both adducts. The acute toxicity tests showed that LD$_{50}$ value for both compounds is 1265 mg/kg, while Effective Dose $_{50}$ for sedation is 531 mg/kg. However, differences were in the onset and lapse of sedation. **Conclusions:** These adducts are bioactive and highly safe agents. Further biological evaluation is desirable to explore medical purposes.

Keywords: boron; carbohydrate; sedation; acute toxicity; adducts; neurons; mice

1. Introduction

Boron-containing compounds (BCC) are interesting molecules in the pharmacological sciences since many of them are bioactive compounds; then, they are attractive for being studied as potential drugs [1]. In particular, some boronic acids are able to easily form di-ester bonds with molecules with hydroxyls, yielding stable boron-containing adducts [2].

In nature, there are some BCC with similar characteristics to those herein reported, such as the fructoborate (Bis[β-D-fructofuranosato(2-)-κ^{2}O^2,O^3]borate), formed by the reaction of two fructose molecules and a boron atom, which is synthesized by plants [3]. Some properties are conferred on that molecule; for example, protective activity against metabolic and inflammatory disorders in

 doi:10.20944/preprints202405.1343.v1

humans. That is a fact supporting that structurally related compounds could be studied as potential drugs [3]. For its part, in animal cells, only compounds presenting cis-diol moieties have been reported as capable of linking to boron-containing moieties [4]. Albeit, if poor knowledge is about the structure-activity relationship of BCCs in animals, it is proposed that when boron is positioned on a biologically active molecule in a donor region, it can generate a potent biological activity because of the strong hydrogen and covalent bonds that these compounds are able to create on target proteins [5].

Also, synthetic procedures to form diols-boronic adducts have been explored. In this sense, some adducts of phenylboronic acid-derived and carbohydrates, and crystals derived from β-fructopyranose [6], α-D-glucofuranose [7] and β-D-arabinopyranose [8] have been reported. The formation of these adducts is interesting, among other facts, due to the disposition of different hydroxyl groups with the feasibility of reacting. In the previously reported structures, the formation of diester bonds has been observed, in a stereoselective reaction, while there is possibility to form several different five or six ring carbohydrates [9]. The applications of these structures are yet to be explored; however, it has been studied in the field of biomaterials for the design of sensors [10]. One of the most promising applications as sensors is for the development of self-regulated insulin delivery materials in the control of glycaemia of patients living with diabetes mellitus [11,12]. Other types of boron-containing monosaccharides have been designed for the overexpression of glucose transporters in brain tumors because of the increased anaerobic metabolism in cancerous cells [13].

It should be mentioned that the toxicity of some BCC has limited studies regarding its biological activity. However, the safety of some other BCC in mammals lets us explore their biological activity and potential to act as drugs [14,15]. As an example is phenylboronic acid, the precursor of the three mentioned compounds. It has a LD_{50} of 900 mg/kg, with i.p. administration in mice [16], but no acute toxicity of their carbohydrate-derivatives has been reported. These facts lead us to evaluate its biological actions as well as the biological activity of these derivatives.

On the other hand, there would be declared the effects on the central nervous system of both, BCC [17,18] and some carbohydrate-derived compounds (for example: topiramate, dapagliflozin), as they have shown multiple biological actions, such as interactions in calcium channels or on enzymes, and exerting some changes which could be involved in some phenomena in neuronal and metabolism functions [19].

In this work, we describe a straightforward one-step synthesis procedure applied for obtaining two carbohydrate-derived BCC. But also, the acute toxicity and sedative effect observed after intraperitoneal administration of these compounds.

2. Materials and Methods

2.1. Materials

2.1.1. Chemicals

D-(-)-Fructose (CAS 57-48-7), D-(-)-Arabinose (CAS 10323-20-3), phenylboronic acid (CAS 98-80-6), acetone (CAS 67-64-1), dimethyl sulfoxide (CAS 67-68-5), dimethylformamide (CAS 68-12-2), acetic acid (CAS 64-19-7), ethanol (CAS 64-17-5), methanol (CAS 67-56-1), butanol (CAS 71-36-3), isopropanol (CAS 67-63-0), ethyl acetate (CAS 141-78-6), chloroform (CAS 67-66-3), dichloromethane (CAS 75-09-2), xylene (CAS 1330-20-7), toluene (CAS 108-88-3), acetaldehyde (CAS 75-07-0), tetrahydrofuran (CAS 109-99-9), carbon tetrachloride (CAS 32488-50-9), acetonitrile (CAS 75-05-8), diethyl ether (CAS 60-29-7), hexane (CAS 110-54-3) and water (CAS 7732-18-5) were obtained from Sigma Aldrich, Merck (St Louis MA, USA). For the Thin Layer Chromatography, the plates used were from TLC Silica gel F_{254} Aluminium sheets (Merck, Germany).

2.1.1. Animals

For the acute toxicity tests, 27 male CD1 mice of 6-7 weeks were employed for each compound for a total of 54 mice. They were obtained from the Vivarium of the Autonomous University of the

 doi:10.20944/preprints202405.1343.v1

State of Hidalgo (*Universidad Autónoma del Estado de Hidalgo, UAEH*). The use of the animals was according to the specifications of the Mexican Official Norm NOM-062-ZOO-1999-SAGARPA, Technic Specifications for the Production, Care and Use of Laboratory Animals. The protocol was approved by the Biosecurity Committee of the Superior School of Medicine of the National Polytechnic Institute (*Escuela Superior de Medicina del Instituto Politécnico Nacional, ESM-IPN*), with the approval code ESM-CBS-01/05-01-2022, 2.0. The animals were disposed in cages of 43 x 53 x 20 cm dimensions with a maximum of 6 mice per cage, at room temperature and with filtered water and rodent food *ad libitum*. The mice had one week for adaptation previous to the study.

2.2. Synthesis and Chemical Characterization

Solubility tests were performed with different solvents, from polar to nonpolar agents. Thin layer chromatography (TLC) was performed to test the reaction process and as a purity criterion. For this test, a mobile phase of hexane/ethyl acetate in a 2:3 proportion was employed. The silica gel TLC plates were cut into a 3x5 cm size, the spots of the compounds to be tested were applied 5 mm above the bottom of the plate, while the limit for the displacement of the mobile phase was 5 mm below the top of the plate. Once the mobile phase was completely dried from the plate, it was analyzed with ultraviolet light to see the displacement of the precursors and the adducts. Then, the Rf value was calculated.

The melting point was measured by using a manual Electrothermal fusiometer by triplicated assay. The Infrared spectra were obtained using a FT-IR Perkin Elmer Frontier spectrometer and a UATR polarizer and are reported as wave number of absorption (cm^{-1}). The Raman spectra were done by placing a sample on a quartz slide, which in turn was placed on a Raman-enhanced microscope (Bruker-Senterra® system, Optik GmbH, Germany). The spectra were obtained by using a laser source of 785 nm, 50 mW power, an integration time of 5 s, and three acquisitions. The resolution was 3–5 cm^{-1}, with a spectral range from 1800 to 440 cm^{-1} and an aperture of 50x100 μm in a 50X objective.

The ^{1}H, ^{13}C and ^{11}B Nuclear Magnetic Resonance spectroscopy was carried out using a Varian Mercury spectrometer operating at 300 MHz, using DMSO-d_6 as solvent. Chemical shifts (δ) are reported in parts per million (ppm) from the residual solvent peak used as reference and coupling constants (J) are at Hz. The following abbreviations are used to indicate the multiplicity s, singlet (s); d, doublet; t, triplet; m, multiplet. X-ray diffraction crystallography was performed using a Bruker APEXII CCD X-ray diffractometer. Mass spectrometry was done using a JEOL The AccuTOF: JMS-T100LC instrument with the DART+ ionization mode.

β-D-fructopyranobisborate (FB-1), ((3aR,5aR,8aR,8bS)-2,7-diphenyltetrahydro-3aH-bis([1,3,2]dioxaborolo)[4,5-b:4',5'-d]pyran-3a-yl)methanol. In a round flask, 1 g (5.55 mmol) of D-(-)-fructose, 1.353 g (11.1 mmol) of phenylboronic acid (1:2 proportion) and 40 mL of acetone were placed. The mixture was stirred and heated to reflux for 180 min, monitored with samples of a silica plaque. The resulting solution was filtered and crystallized by nucleation, changing the cooling rate. Crystals were observed after 2 days to obtain 1.498 g (4.26 mmol) of **FB-1** in 76.75% yield as a white powder, M.P. 94±1°C; IR νmax (cm^{-1}): 1028, 1219, 1499, 1603, 1739, 2971, 3384. Raman shift (cm^{-1}): 1001, 1577, 1604, 3064, 3347. ^{1}H NMR (300 MHz) δ 7.72 (dd, *J* = 12.9, 6.5, 28H), 7.48 (dd, *J* = 15.4, 8.0, 13H), 7.43 – 7.28 (m, 30H), 5.13 (s, 1H), 4.47 (dt, *J* = 9.1, 4.7, 1H), 4.36 (dd, *J* = 5.9, 2.6, 1H), 4.31 (d, *J* = 3.6, 1H), 4.22 (dd, *J* = 2.9, 2.2, 1H3), 3.92 (dd, *J* = 8.9, 3.3, 1H), 3.40 (dd, *J* = 12.1, 1.8, 1H), 3.24 (dd, *J* = 11.1, 5.2, 1H). ^{13}C NMR (75 MHz, DMSO-d_6) δ 135.05 (C17, C21), 134.52 (C22, C26), 132.33 (C12, C16), 128.52 (C18, C20), 128.49 (C20), 127.86 (C23), 127.78 (C25), 97.17 (C4), 72.62 (C6), 72.15 (C5), 72.12 (C1), 72.09 (C2), 60.26 (C10). ^{11}B NMR (96 MHz) δ 33.64. MS m/z 370 [M + H20]+. See supplementary material for spectra.

β-D-arabinopyranobisborate (AB-1): I(3aR,5aR,8aR,8bS)-2,7-diphenyltetrahydro-5H-bis([1,3,2]dioxaborolo)[4,5-b:4',5'-d]pyran. Synthesized as described for FB-1 but starting from 0.833 g of D-(-)-Arabinose (5.55 mmol), 1.353 g of phenylboronic acid (11.1 mmol) and 40 mL of acetone to obtain 1.251 g (3.89 mmol) of AB-1 in 70.05% yield as a white powder, M.P. 160±1°C; IR νmax (cm^{-1}): 1026, 1218, 1497, 1602, 1739, 2971. Raman shift (cm^{-1}): 998, 1574, 1605, 3057, 3406. ^{1}H NMR (300

 doi:10.20944/preprints202405.1343.v1

MHz, dmso) δ 7.79 – 7.69 (m, 9H), 7.56 – 7.43 (m, 5H), 7.42 – 7.32 (m, 9H), 5.32 (d, *J* = 1.8, 1H), 4.71 (d, *J* = 2.6, 2H), 4.49 (d, *J* = 2.4, 1H), 4.26 (d, *J* = 10.1, 3H), 3.74 (dd, *J* = 11.6, 3.4 Hz, 2H), 3.37 (dd, *J* = 9.8, 2.4, 2H). ^{13}C NMR (75 MHz, DMSO-d_6) δ 135.20 (C7, 14), 133.96 (C15, C19, C20, C24), 132.47 (C17), 131.42 (C22), 128.46 (C16, C18), 128.07 (C21, C23), 115.23 (C9), 86.22 (C10), 74.99 (C2), 74.52 (C1), 63.19 (C6). ^{11}B NMR (96 MHz) δ 29.02. MS m/z 323 [M]+. See supplementary material for spectra.

2.3. Single Crystal X-ray Molecular Structure

Single crystals of **FB-1** and **AB-1** suitable for X-ray diffraction, were obtained from saturated solutions of acetone. **FB-1** crystallized with one molecule of acetone. The monocrystal data of BCCs were recorded on a Bruker D8 VENTURE diffractometer using a graphite monochromator (Mo Kα, λ = 0.71073 Å) at 185(2) K. The SAINT [20] and SORTAV software [21] were used to carry out the cell refinement and data reduction, respectively. The structures were solved by direct methods using the SHELXS-97 program [22] of the WINGX package [23]. The full-matrix least-squares methods were used to perform the final refinement with the SHELX97 program [22]. The H atoms on C, N, and O were geometrically positioned and treated as riding atoms with: C–H = 0.93-0.98 Å, Uiso(H) = 1.2 eq(C) for aromatic carbon atoms. Figures for publication were prepared with Platon [24]and Mercury [25]. General crystallographic data for compounds **FB-1** and **AB-1** were deposited in the Cambridge Crystallographic Data Centre (CCDC) as supplementary publication numbers 2351428 and 2351427, respectively.

2.4. In-Silico Prediction of the Physicochemical Properties

Given the fact these compounds have not been tested yet, we made use of some online servers, such as Protox II [26], SwissADME [27], SwissTarget [28] and Molinspiration [29] to predict some of their physicochemical properties as well as putative target [30,31].

2.5. Biological Evaluation

For the acute toxicity tests, modified Lorke's method was employed [32]. In brief, in the first phase, three groups of the mice were established with a value of n=3 with different doses: 10, 100 and 1000 mg/kg body weight administered intraperitoneally in a single dose. The second phase involved the formation of five different groups with n=3 using new doses, depending on the results of the first phase. The doses were 140, 225, 370, 600 and 1600 mg/kg body weight intraperitoneally in a single dose. The median lethal dose (LD_{50}) was obtained by calculating the geometric mean between the dose value where none of the mice survived and the last dose where all the mice lived.

Additionally, due to preliminary tests showing a sedative effect by administering doses higher than 100 mg/kg of the compounds, a test to define the median effective dose (ED_{50}) for hypnosis and sedation for both compounds was set up. The same scheme from the second phase of Lorke's method was used for this purpose. Five different doses were put in the animals. The doses established were 140, 225, 370, 470 and 600 mg/kg body weight intraperitoneally in a single dose. The animals were examined for the first 2 hours, and then, 6, 12, 24, 48 and 72 hours after the administration of the compounds. The visual evaluation of the behavior of the mice was the tool to recognize if they presented hypnosis or sedation, as described by Bin et al. [33]. For hypnosis, the righting (recovering from being positioned on its side) should be more than 10 seconds but less than 60 seconds; for sedation, the righting should be more than 60 seconds, or, by default, if they go asleep. The analysis of this test was carried out with a probit and logit curve.

Open field test was carried out 5 min before treatments to discard any motor disturbance affecting performance. In brief, mice were placed into motor activity measuring cages (50x50x50 cm, with detectors each 2.5 cm, OA-BioMed OMNIALVA®, Mexico) for determining the total number of movements, distance traveled, highest speed, and vertical movements as elsewhere [34]; This evaluation was repeated at 0.25 0.5, 1, 2, 6, 12, 24, 48 and 72 h after treatment.

3. Results

 doi:10.20944/preprints202405.1343.v1

3.1. Chemistry

The synthesis of the BCC adducts was performed by condensation between the sugar and phenylboronic acid in 1:2 proportion in acetone under very mild conditions. The straightforward one-step synthesis procedure is depicted in Figure 1. Crystals were created after 2 days, then, all the characterization tests were performed. Both the fructophenylborate adduct (**FB-1**) and the arabinophenylborate (**AB-1**) have a transparent, crystalline and geometric aspect, forming crystals of approximately 5x2 mm for **FB-1** and 3x1mm for **AB-1**. The yields were 76% for **FB-1** and 70% for **AB-1**. When it comes to solubility, **FB-1** is soluble in alcohols (methanol, ethanol, isopropanol and butanol), while **AB-1** does not show to be soluble. The compounds were not completely pure, then purification was performed in order to remove the starting material (phenylboronic acid and saccharides): the extraction of the saccharides was considerably easy by washing with distilled water. The carbohydrates are soluble but both FB-1 and AB-1 are not. For the phenylboronic acid purification, the process for FB-1 was a major challenge: FB-1 had the same solubility as phenylboronic acid in almost all the solvents used. It only was soluble in dichloromethane and phenylboronic acid was not, so that the dissolved adduct had to pass through a Rotavapor to evaporate the dichloromethane; for AB-1, ethanol was useful because of the insolubility of AB-1 in alcohols, while phenylboronic acid was completely soluble. In order to recrystallize to get some x-ray diffraction quality level crystals, both adducts were dissolved once again in acetone and let the solvent slowly evaporate.

In the Thin Layer Chromatography, the Rf value for FB-1 was 0.42, while the Rf value for AB-1 was 0.49, employing a mobile phase of hexane/ethyl acetate in a 2:3 proportion. There was no evidence that the precursors left a spot in the same line where the products were positioned.

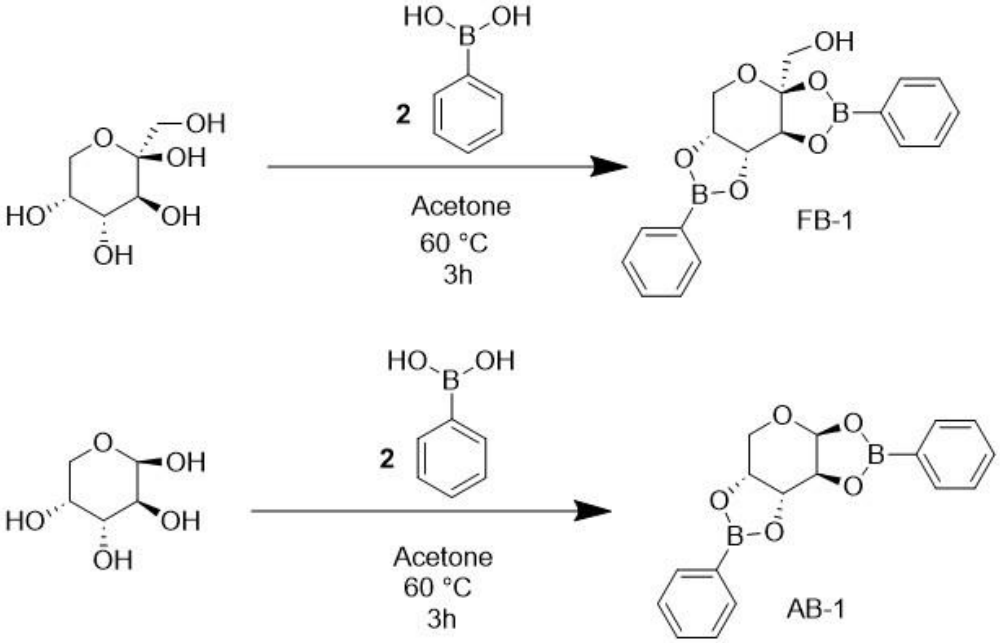

Figure 1. Scheme of the synthesis reaction for the carboboronic compounds. Each carbohydrate equivalent requires 2 equivalents of phenylboronic acid to generate two diester bonds for the new adducts.

3.3. X-ray Diffraction Crystallography

The compounds crystallized accurately to develop this study. The compounds were illustrated in the Oak Ridge Thermal Ellipsoid Plot (ORTEP) diagrams of Figures 2 and 3.

 doi:10.20944/preprints202405.1343.v1

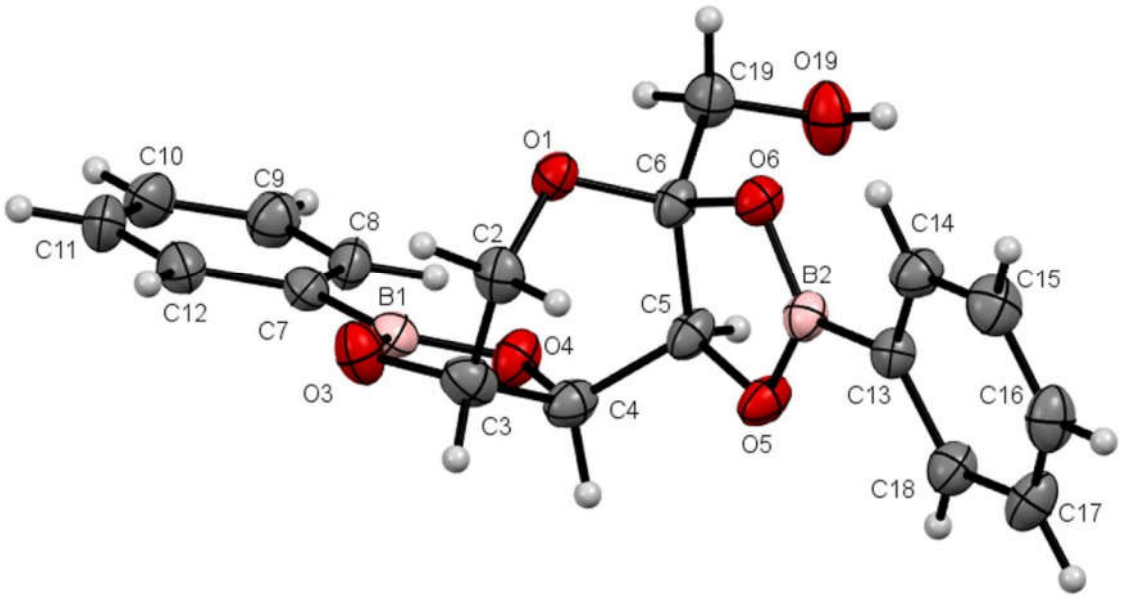

Figure 2. ORTEP diagram of the β-D-fructopyranoborate (**FB-1**), the acetone molecule was omitted for clarity.

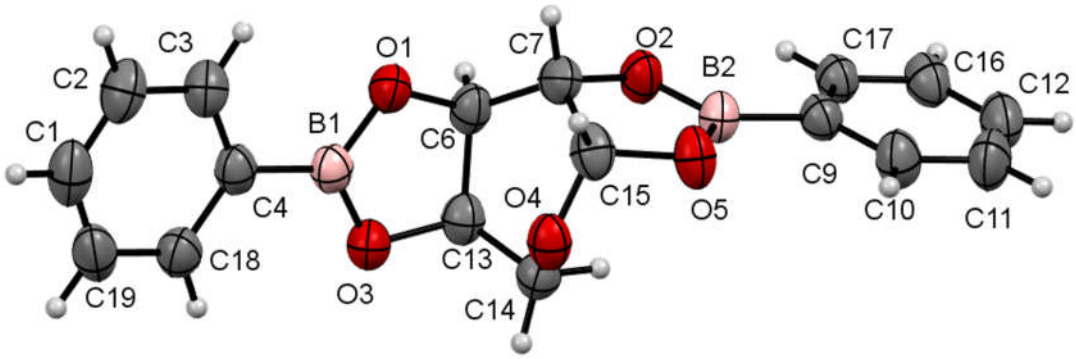

Figure 3. ORTEP diagram of the β-D-arabinopyranoborate (**AB-1**).

3.4. In-Silico Predictions

On the Protox II server, the predicted LD_{50} for **AB-1** was 180 mg/kg, with a toxicity class of 3, while for **FB-1,** LD_{50} was predicted of 1000 mg/kg with a toxicity class of 4 (See supplementary material).

The SwissADME server showed a LogP of 0.33 for **AB-1**, and the Egan graphic showed a high absorption by the gastrointestinal tract; while for **FB-1**, a LogP of -0.30, and the Egan graphic showed high absorption the gastrointestinal tract.

The Molinspiration server predicted a LogP of 2.26 for **AB-1** and a TSPA value of 46.17; while for **FB-1**, a LogP of 1.7 and a TSPA value of 66.4. Both servers predicted no violation of the Lipinski rule of 5 for both compounds.

The SwissTarget server pointed out the following results: for AB-1, there is a 33.3% chance of binding to a Family A G protein-coupled receptor, and another 33.3% of binding to enzymes. The most related targets are types II, I, XII and IX Carbonic anhydrases, the phenylalanyl-tRNA synthetase mitochondrial, the estrogen receptor beta, the A1, A2a, A2b, the A3 receptors, the endothelium receptor ET-A, the hexokinase type IV, the alkaline phosphatase, tissue-nonspecific isoenzyme, the bifunctional protein NCOAT and the arachidonate 15-lipoxygenase. For FB-1, there

 doi:10.20944/preprints202405.1343.v1

is a 33.3% chance of binding to a Family A G protein-coupled receptor, a 13.3% chance of binding to electrochemical transporters, and 13.3% chance of binding to proteases; the main targets are A1, A2a, A3 and A2b adenosine receptors, ADAM17, the bifunctional protein NCOAT, hexokinase type IV, transmembrane domain-containing protein TMIGD3, the protein kinase C alpha, thymidine kinase, cytosolic, the butyrylcholinesterase, the matrix metalloproteinase 13, and the sodium/glucose cotransporter type 2 and 1.

3.5. Acute Toxicity Test

In the first phase of the acute toxicity test by Lorke's method, three mice for each of the three doses were employed. For both **FB-1** and **AB-1**, all the mice in the three groups survived, despite the dose applied (10, 100 and 1000 mg/kg body weight).

For the second phase, a single 1600 mg/kg BW I.P. dose for each of the products was implemented (using three mice for each compound), showing that the two animals of both groups did not survive. The geometric mean was calculated between the doses of 1000 mg/kg (the last dose where all the mice survived) and 1600 mg/kg (the first dose where all the mice died), obtaining a median lethal dose (LD_{50}) of 1265 mg/kg for both **FB-1** and **AB-1**.

3.6. Determination of the Median Effective Dose (ED_{50}) for Hypnosis and Sedation

With the first phase used in the acute toxicity test, it was observed that in the 1000 mg/kg dose, both mice administered with **FB-1** and **AB-1** fell asleep, while the mice from the 10 and 100 mg/kg doses had no behavioral impairment. The doses established for the second phase were 140, 225, 370, 470 and 600 mg/kg, applying to three mice for each dose for each compound.

In both groups, hypnosis signs were observed in the 470 mg/kg dose. The ED_{50} for hypnosis was calculated by the Probit curves, obtaining a dose of 417 mg/kg.

As seen in the hypnosis test, the sedation test had similar results for both compounds studied. The sedation signs were observed in the 600 mg/kg dose. The estimated ED_{50} for sedation was 531 mg/kg.

Additionally, motor evaluation was performed as a complement to the visual evaluation of sedation and hypnosis since it allows you to observe diminished activity after **FB-1** or **AB-1** administration (Figures 4-6). As it is notable in the plots, **FB-1** administration (at doses ≥370 mg/kg) induced sedation and diminished motor activity before the first hour and recovery at 6 h; while for **AB-1** administration (at doses ≥225 mg/kg) induced sedation and diminished motor activity before the first hour and recovery at 6 to 72 h (in dose-dependence).

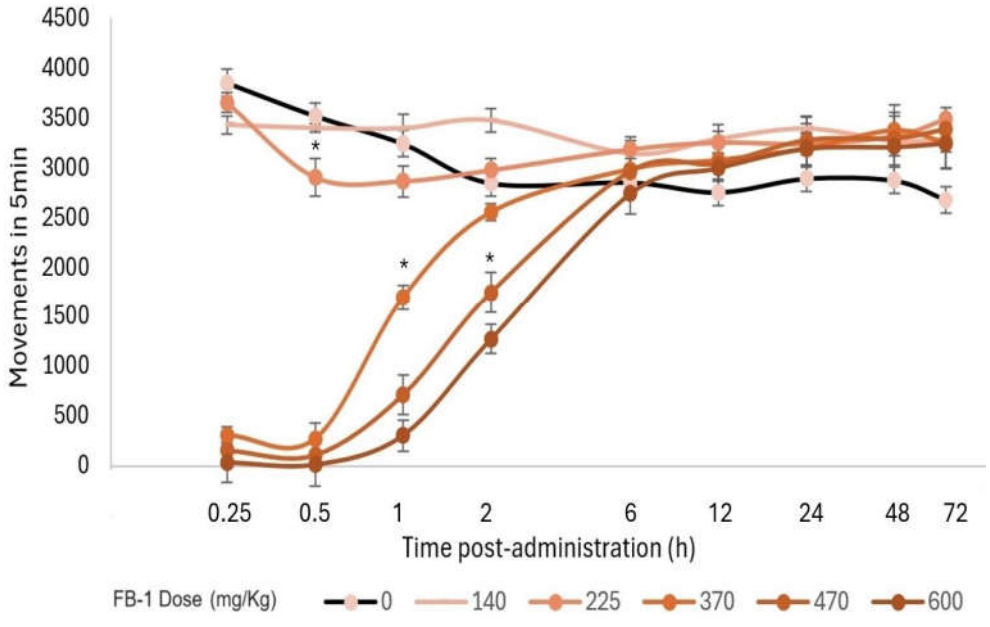

Preprints.org (www.preprints.org) | NOT PEER-REVIEWED | Posted: 21 May 2024 doi:10.20944/preprints202405.1343.v1

Figure 4. Motor performance in the open field test. Motor activity in 5 minutes, and the effect on locomotion after **FB-1** administration. The markers represent the mean, while bars are for standard error of mean. An asterisk is in the lowest dose which in each measured time diminished the total of movements compared to the control group, $p < 0.05$; $n \geq 4$.

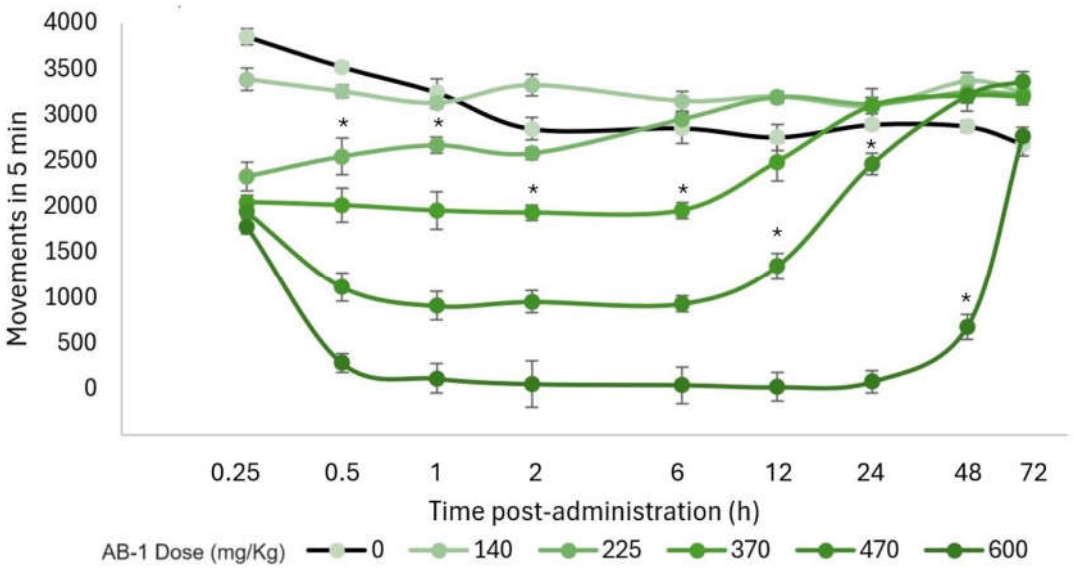

Figure 5. Motor performance in the open field test. Motor activity in 5 minutes, and the effect on locomotion after **AB-1** administration.The markers represent the mean, while bars are for standard error of mean. An asterisk is in the lowest dose which in each measured time diminished the total of movements compared with the control group, $p < 0.05$; $n \geq 4$.

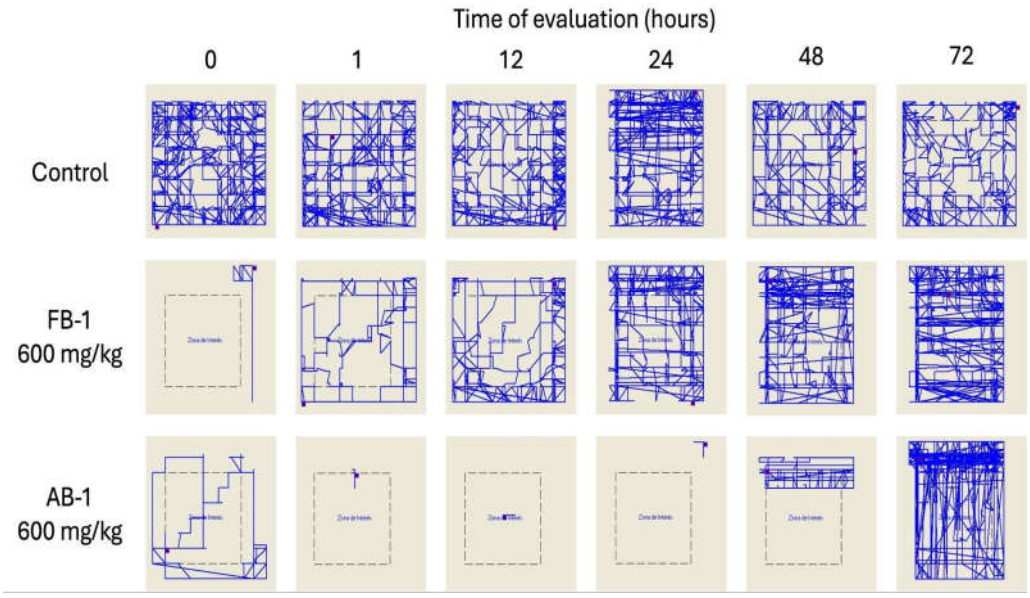

Figure 6. Motor performance in the open field test. Illustrative reports of effects by administration of FB-1 or AB-1 (in the highest tested doses).

4. Discussion

Two BCCs were synthesized and analyzed in extensive form for first time; one using D-fructose and the other from D-arabinose, both with phenylboronic acid as the boron compound precursor. The synthesis reaction allowed a yield higher than 70%, with a reduced waste of the reagents employed. Although the method used to synthesize the boron-carbohydrate adducts in our

 doi:10.20944/preprints202405.1343.v1

laboratory was different to the previously reported [6,8], mainly in the use of different solvents and the recrystallization techniques, the products were obtained with the same macroscopic characteristics.

The thin layer chromatography tests showed that the products obtained had a different Rf value than the carbohydrates (and phenylboronic acid, supporting the formation of new products). The melting point for the products was different from the one reported for the used reagents. There have been reported some borates capable of transferring hydrophilic molecules (like saccharides) across the cell membrane because of their high lipophilicity [35–37].

The Infrared and Raman spectra were complementary and pointed out characteristic signals in the spectra; in **FB-1**, the stretching of O-H bonds was observed at a wavelength of 3400 cm^{-1}, C-H at 3000 cm^{-1}, the signals corresponding to the B-O bonds in 1500 cm^{-1} and the signals for the phenyl group in 1300 cm^{-1}. All the signals were also presented in the Raman and the Infrared spectra for **AB-1**, with the exception for the O-H stretching signal at 3400 cm^{-1}, and that is justified by the fact that, with the formation of the diester bonds, new B-O bonds are formed, so the new compound have no hydroxyl groups and the signal for this structure is missing, which is completely expected.

The ^{1}H NMR spectra of both compounds showed signals in the range of 7-8 ppm corresponding to the protons in the aromatic rings. The most important signals are those involving the carbon atoms where the diester bonds were formed. The anomeric carbon of the carbohydrate ring in the β-D-fructopyranoborate (**FB-1**) has no proton, so it does not produce any signal by itself. The proton of the carbon in position 2 has one vicinal proton in *trans* position, the *J* value is 3.6 Hz with a double signal, and it appears in the δ4.31; the proton linked to the carbon of position 3 has two different vicinal protons, one in *trans* and the other in *cis* position, getting two different *J* values of 5.9 Hz and 2.6 Hz, with a double doublet because of the unfolding signals; the proton in the carbon of position 4 has one vicinal proton in *cis* position, but is linked to a methylene group, with two protons in positions, getting a triple doublet signal with a *J* value of 9.1 Hz and 4.7 Hz.

The ^{1}H NMR spectra of the β-D-arabinopyranoborate (**AB-1**) has a special feature because it lacks the hydroxymethyl presented in the previous compound (the fructose is a hexose, while the arabinose is a pentose), so the anomeric carbon has a proton, and it produces a signal in this spectrum, this is double and the vicinal proton is in *cis* position, so the *J* value is of 5.0 Hz. The interesting fact is that, the proton linked to the carbon in position 2 now has two vicinal protons with different *J* values because one proton is in *trans* position, while the other one is in a *cis* position, and the unfolding signals because of the two different *J* values generates a double doublet. The only way this can be possible is that, when the D-arabinose formed a ring, it had to be in the β-anomer, because it allows the oxygen linked to carbons in position 1 and 2 to place in the same plane, so the reaction for the formation of the diester bond is in *cis* position (it is necessary to remind that the diester bonds are not possible if the oxygens are in *trans* position). With the Karplus equation, we could confirm from the Φ torsion angles the *J* value the *J* values of the *cis* and *trans* disposition of the protons involved [38]. The vicinal protons with a *cis* position have an angle from 0 to 90° with a lower *J* value (2.5-3.2 Hz), while the *trans* vicinal protons have a 90 to 180° torsion angle, with a greater *J* value (5.0 ± 1 Hz) [39].

If the carbohydrate had closed itself in an α anomer, one of the two diester bonds formed in the new adducts could not be formed. When monosaccharides are dissolved in aqueous solution, they form different isomers of 6 and 5 membered rings with α and β anomers; some carbohydrates like fructose are more likely to bind to boronic acids than others like glucose, because the fraction of the isomers with syn hydroxyl groups is higher in fructose (nearly 25%) than in glucose (1%) [40].

Regarding the formation of 1,3 and 1,4-diols cyclic boronic esters of 5,6 or 7 membered rings, with enhanced N-B interactions, some authors established the mechanisms by which boronic acids are able to bind some saccharides, and once linked, the pH drop change in these compounds modulates the fluorescence of certain fluorophores, making possible the identification of specific carbohydrates [41–44]. However, those works mentioned the effect in the N-B bonds from the interaction of BCCs with molecules which can form 1,3 and 1,4-diols. Anyway, the unique interaction reported in the binding to carbohydrates is with furanoses, like D-fructofuranose, where the boronic

 doi:10.20944/preprints202405.1343.v1

acid generates a 2,3-cis-diol with the furanose, but the 4,5-diol is not formed because the hydroxyl groups are in *trans* position [45]. With the analysis of this work, we proposed that the cyclization of a D-fructopyranose and a D-arabinopyranose allows the formation of two diols for each saccharide molecule.

The ^{13}C NMR spectra gives us relevant information to confirm the presence of a specific anomer formed in the synthesis reaction. In the range of 90-100 ppm of the ^{13}C NMR spectrum, there are presented signals corresponding to the anomeric carbon, α or β [46]. In the case of both carbohydrate-derived boron adducts, there is observed just one signal in the range previously mentioned, which means only one anomer is being formed after the synthesis reaction. Just by itself, this result cannot give more information about whether the anomer formed in the synthesis reaction is α or β; however, the ^{1}H NMR spectra previously analyzed had indirectly proven the cyclization as a β-anomer.

The X-ray diffractions of both compounds were possible because the crystals obtained had an accurate crystalline and geometric appearance that allows to diffract correctly for this technique; this study could confirm what was already observed in the previously mentioned spectroscopy techniques: the new carbohydrate-derived boron compounds are formed by the cyclization of the carbohydrate in a β-pyranose, and formed two diester bonds with two molecules of phenylboronic acid: a 2,3-*cis*-diol and 4,5-*cis*-diol for **FB-1**; and 1,2-*cis*-diol and a 3,4-*cis*-diol for **AB-1**. The position of the two oxygens in each diester bond is in the same plane, so the reaction was in *cis* position.

The D-fructose equilibrium in water shows that, the pyranose form is the most favorable when cycling with a 72%, while the furanose proportion is of 28%; the β-anomer have a proportion on 70% in pyranoses, and 23% in furanoses, being the predominant anomer [47]. For the formation of FB-1, the most predominant isomer, the β-fructopyranose, is ideal because it allows the binding of two equivalents of phenylboronic acid, forming two diester bonds. There is not enough information about the isomer forms of D-arabinose in aqueous solutions, but it is well described in L-arabinose that the α-anomer have a higher proportion in the non-polar solvents, obeying the anomeric effect; while the cyclization could be variable depending on the solvent, being up to 33% in dimethyl sulfoxide and only 3 % in deuterated water in the furanose form; at least with these two solvents reported, it seems that the pyranose form tends to be the dominant proportion [48]. The acetone used in the synthesis is a polar solvent, then, it is expected to find a higher proportion of the β-anomer, going against what the anomeric effect dictates for both compounds.

It is possible that the α-anomer could also be formed in the synthesis reaction, but the proportion is not enough to generate any significant signal. The absence of the anomeric effect could explain this phenomenon: it is possible that more than 95% of the new synthesized compound is closed as a β-anomer; nevertheless, once the β-anomer is used, the proportion of the α-anomer is higher, so an interconversion of anomers happens in order to maintain the proportion of 95% β-anomer and 5% α-anomer. Therefore, the anomeric effect does not happen in this reaction as expected for a hexopyranose, just like what is observed with the glucose.

It was observed that the mice with the 1000 mg/kg body weight dose got sedated after 5 minutes of administration and this effect lasted for about 2 hours for **FB-1**, and it lasted until 72 hours after administration for the **AB-1**; after that time, the mice could recover completely, and they had not any neurological or motor complication. With the dose of 1600 mg/kg body weight, the mice got sedated in the first 3-5 minutes of administration. However, they did not survive after 5 to 6 hours. The LD_{50} higher than 1200 mg/kg for both compounds allows us to declare these products safe to be administered. It is intriguing the fact that phenylboronic acid has a LD_{50} of 900 mg/kg, considerably lower than that calculated for the adducts; but being the precursor of these products and with its structure almost intact, presents less acute toxicity. The two hydroxyl groups in the phenylboronic acid are replaced by the cys-diol unions with the saccharides. Both the saccharide and the borate precursor have lost their most polar component (the hydroxyl groups), so that the new compounds are significantly more non-polar (**FB-1** has just one hydroxymethyl, while **AB-1** completely lacks hydroxyls). Then, due to lipophilic profile they increased the chance to cross the blood-brain barrier (BBB). That would be related to the triggered hypnosis and sedation, both neurological effects.

 doi:10.20944/preprints202405.1343.v1

The hypnosis and sedation effects observed in both compounds led us to review the properties of the compounds and the implications in a therapeutic manner: the study of the effective dose 50 is the beginning of this extension of the protocol in order to establish safe doses for forward clinical studies as is usually determined with new drugs [49].

The mechanism of action is unclear, however, *in-silico* predictors suggest, in this sense, compounds with carbohydrate structures and some BCC have been reported as sedative: some well-known benzodiazepines, like alprazolam, have been tested to form some complexes with boric acid and boronic acids have been crystallized [50]. Alprazolam works by binding to the GABA-A receptor, increasing the activity of γ-aminobutyric acid (GABA), an inhibitory neurotransmitter [51]. Boric acid was named "sedative salt" after being isolated from borax by Wilhelm Holmberg in 1702 [52]. Nonetheless, there was observed a toxic effect of this sedative salt, resulting in the death of various people, mainly children, the reason why its use was disrupted for those purposes [53–57].

Another drug utilized nowadays with a possible effect on the gabaergic activity is topiramate [58]. Its structure has a main 6-membered ring fructose [59]. Other mechanisms of action have been described for this antiepileptic, such as the blockage of the voltage-dependent sodium channels [60], the negative modulatory effect on the L-type calcium channels [61], the inhibition of the carbonic anhydrase isoforms [62], and the antagonism of the N-methyl-D-aspartate glutamate receptor [63]. The structure of topiramate is clearly similar to that observed for the adducts presented in this work, particularly for FB-1, so, it is hypothesized that the similarity in their structures confers them similarity in their biological activities, and maybe they share protein targets.

Even though both synthetic compounds have the same ED_{50} for hypnosis and sedation, the clinical effects observed were significantly different. For **FB-1**, the beginning of the behavior impairment was 5 minutes after administration, while **AB-1** triggered the effects 10 to 15 minutes later. The most important finding was the duration of the sedative effects: **FB-1** lasted about 60 minutes for hypnosis and 2 hours for sedation, while **AB-1** had a hypnosis effect of more than 5 hours, and for sedation, the effect lasted up to 72 hours. The animals had to be strictly observed because the prolonged effect could be dismissed because the mice could not feed by themselves. In order to avoid death from starvation, they were fed by the lab personnel until the full recovery of the rodents.

Limitations of our study include the requirement to use 5 % DMSO solution as a vehicle, due to poor solubilization of the compounds in water or saline solution. Also, the administration was intraperitoneal, while oral administration would allow better comparison to other well-known sedative drugs, like topiramate.

Another limitation was in the clear elucidation of the mechanism of action, albeit the high structural homology of the topiramate and the tested adducts, since topiramate has multiple mechanisms of action. Moreover, there are other possible mechanisms why this phenomenon occurs. For example, the kinetic behavior of adducts could release sugars and phenylboronic acid, or other unknown metabolites inducing observed biological effects.

Further studies are required to elucidate the mechanism(s) of action, and if the pharmacodynamic and pharmacokinetic profiles of these two compounds are related to the observed induced changes. Also, for studying potential applications in neurological disorders. In addition, it is interesting to study these compounds in mammals (temperature, pH) physiological conditions to propose application in their pathologies, but also if their biotransformation could release bioactive compounds and modify the carbohydrate metabolisms.

5. Conclusions

Two carbohydrate-derived BCC were obtained by a simple one-step procedure. Diester bonds were formed with two hydroxyls in a *cis* position. The stereoselective reaction has been demonstrated by different spectroscopy techniques, and also by X-ray diffraction crystallography.

Additionally, it was described that these compounds are less toxic than their boron-containing precursor (phenylboronic acid), estimating a LD_{50} for both compounds of 1265 mg/kg. Notably, a sedative action was observed after their administration, being effective in doses higher than 100 mg/kg. The sedative effect is dose-dependent, and its duration is different between two BCC.

 doi:10.20944/preprints202405.1343.v1

Additional approaches are required to explore the mechanism of action and pharmacokinetics of these BCCs.

Supplementary Materials: The following supporting information can be downloaded at the website of this paper posted on Preprints.org. Fig S1. Raman spectra comparison of phenylboronic acid, β-D-fructopyranoborate (FB-1), and β-D-arabinopyranoborate (AB-1); Fig S2. IR-FT spectrum of the β-D-fructopyranoborate (FB-1); Fig S3. IR-FT spectrum of the β-D-arabinopyranoborate (AB-1); Fig S4. ^{1}H RMN (DMSO-d_6, 300 MHz) of the β-D-fructopyranoborate (FB-1); Fig S5. ^{13}C RMN (DMSO-d_6, 76.5 MHz) of the β-D-fructopyranoborate (FB-1); Fig S6. ^{11}B RMN (DMSO-d_6, 96 MHz) of the β-D-fructopyranoborate (FB-1); Fig S7. ^{1}H RMN (DMSO-d_6, 300 MHz) of the β-D-arabinopyranoborate (AB-1); Fig S8. ^{13}C RMN (DMSO-d_6, 76.5 MHz) of the β-D-arabinopyranoborate (AB-1); Fig S9. ^{11}B RMN (DMSO-d_6, 96 MHz) of the β-D-arabinopyranoborate (AB-1); Fig S10. Prediction in the Protox II server for the β-D-fructopyranoborate (FB-1); Fig S11. Prediction in the Protox II server for the β-D-arabinopyranoborate (AB-1); Fig S12. Prediction in the SwissADME server for the β-D-fructopyranoborate (FB-1); Fig S13. Prediction in the SwissADME server for the β-D-arabinopyranoborate (AB-1); Fig S14. Prediction in the Molinspiration server for the β-D-fructopyranoborate (FB-1); Fig S15. Prediction in the Molinspiration server for the β-D-arabinopyranoborate (AB-1); Fig S15. Prediction in the Molinspiration server for the β-D-arabinopyranoborate (AB-1); Fig S16. Prediction in the SwissTarget server for the β-D-fructopyranoborate (FB-1); Fig S17. Prediction in the SwissTarget server for the β-D-arabinopyranoborate (AB-1).

Author Contributions: R.I.C.-C., J.G.T.F., and M.A.S.-U.: Conceptualization. R.I.C.-C., H.G-E., A.A-.G., E.D.F.-G., C.O.-C., A.C.-R. and M.A.S.-U.: participated in the methodology procedures, R.I.C.C, I.I.P.-M., J.G.T.-F. and M.A.S.-U.: participated in the formal analysis; R.I.C.-C., and M.A.S.-U.:. wrote the original draft. All authors have read, edited and agreed to the final version of this manuscript.

Funding: This work was supported by Secretaría de Investigación y Posgrado del Instituto Politécnico Nacional (SIP-M2303), and Consejo Nacional de Ciencia y Tecnología.

Institutional Review Board Statement: The biological evaluation is in agreement with Mexican National Research Council specifications for the production, care, and use of laboratory animals and the use of some species inside the laboratory. The protocol was approved by the Biosecurity Committee of the Superior School of Medicine of the National Polytechnic Institute (*Escuela Superior de Medicina del Instituto Politécnico Nacional, ESM-IPN*), with the approval code ESM-CBS-01/05-01-2022, 2.0.

Informed Consent Statement: Not applicable.

Data Availability Statement: Any complementary data of the reported data are available on request from the corresponding authors.

Acknowledgments: Authors thank the financial support by Secretaría de Investigación y Posgrado del Instituto Politécnico Nacional (IPN), the Consejo Nacional de Humanidades, Ciencias y Tecnologías (CONAHCyT) and the Programa Institucional para la Formación de Investigadores (PIFI). Authors also thank to Adriana Lizbeth Rivera Espejel for helping us to perform Mass spectrometry at the Instituto de Química de la Universidad Nacional Autónoma de México.

Conflicts of Interest: The authors declare no conflicts of interest.

References

1. Grams, R. J., Santos, W. L., Scorei, I. R., Abad-García, A., Rosenblum, C. A., Bita, A., Cerecetto, H., Viñas, C., & Soriano-Ursúa, M. A. (2024). The Rise of Boron-Containing Compounds: Advancements in Synthesis, Medicinal Chemistry, and Emerging Pharmacology. *Chemical reviews*, *124*(5), 2441–2511. https://doi.org/10.1021/acs.chemrev.3c00663.
2. Baker, S. J., Ding, C. Z., Akama, T., Zhang, Y. K., Hernandez, V., & Xia, Y. (2009). Therapeutic potential of boron-containing compounds. *Future medicinal chemistry*, *1*(7), 1275–1288. https://doi.org/10.4155/fmc.09.71.
3. Hunter, J. M., Nemzer, B. V., Rangavajla, N., Biţă, A., Rogoveanu, O. C., Neamţu, J., Scorei, I. R., Bejenaru, L. E., Rău, G., Bejenaru, C., & Mogoşanu, G. D. (2019). The Fructoborates: Part of a Family of Naturally Occurring Sugar-Borate Complexes-Biochemistry, Physiology, and Impact on Human Health: a Review. *Biological trace element research*, *188*(1), 11–25. https://doi.org/10.1007/s12011-018-1550-4.
4. Ban, H. S., & Nakamura, H. (2015). Boron-Based Drug Design. *Chemical record (New York, N.Y.)*, *15*(3), 616–635. https://doi.org/10.1002/tcr.201402100.

5. Hunt C. D. (2012). Dietary boron: progress in establishing essential roles in human physiology. *Journal of trace elements in medicine and biology : organ of the Society for Minerals and Trace Elements (GMS)*, *26*(2-3), 157–160. https://doi.org/10.1016/j.jtemb.2012.03.014.
6. Draffin, S. P., Duggan, P. J. & Fallon, G. D. (2004). O2,O3:O4,O5-Bis (phenylboranediyl)-β-D-fructo-pyranose acetone solvate. *Acta Crystallographica. 60*: 1520-1522. https://doi.org/10.1107/S1600536804019245.
7. Draffin, S. P., Duggan, P. J., Fallon, G. D. & Tyndall, E. M. (2005). O1,O2:O3,O5 - Bis (phenylboranediyl)-α-D-glucofuranose. *Acta Crystallographica. 61*: 1733-1735. https://doi.org/10.1107/S1600536805014480.
8. Reichvilser, M. M., Heinzl, C., & Klüfers, P. (2010). Boronic acid mono- and diesters of the aldopentoses. *Carbohydrate research*, *345*(4), 498–502. https://doi.org/10.1016/j.carres.2009.11.022.
9. Wu, X., Li, Z., Chen, X. X., Fossey, J. S., James, T. D., & Jiang, Y. B. (2013). Selective sensing of saccharides using simple boronic acids and their aggregates. *Chemical Society reviews*, *42*(20), 8032–8048. https://doi.org/10.1039/c3cs60148j.
10. Brooks, W. L. A., Deng, C. C., & Sumerlin, B. S. (2018). Structure-Reactivity Relationships in Boronic Acid-Diol Complexation. *ACS omega*, *3*(12), 17863–17870. https://doi.org/10.1021/acsomega.8b02999.
11. Banach, Ł., Williams, G. T. & Fossey, J. S. (2021). Insulin Delivery Using Dynamic Covalent Boronic Acid/Ester-Controlled Release. *Adv. Therap*. 2100118. https://doi.org/10.1002/adtp.202100118.
12. Mohanty, A. R., Ravikumar, A., & Peppas, N. A. (2022). Recent advances in glucose-responsive insulin delivery systems: novel hydrogels and future applications. *Regenerative biomaterials*, *9*, rbac056. https://doi.org/10.1093/rb/rbac056.
13. Itoh, T., Tamura, K., Ueda, H., Tanaka, T., Sato, K., Kuroda, R., & Aoki, S. (2018). Design and synthesis of boron containing monosaccharides by the hydroboration of d-glucal for use in boron neutron capture therapy (BNCT). *Bioorganic & medicinal chemistry*, *26*(22), 5922–5933. https://doi.org/10.1016/j.bmc.2018.10.041.
14. Soriano-Ursúa, M. A., Farfán-García, E. D., & Geninatti-Crich, S. (2019). Turning Fear of Boron Toxicity into Boron-containing Drug Design. *Current medicinal chemistry*, *26*(26), 5005–5018. https://doi.org/10.2174/0929867326666190327154954.
15. Farfán-García, E. D., Castillo-Mendieta, N. T., Ciprés-Flores, F. J., Padilla-Martínez, I. I., Trujillo-Ferrara, J. G., & Soriano-Ursúa, M. A. (2016). Current data regarding the structure-toxicity relationship of boron-containing compounds. *Toxicology letters*, *258*, 115–125. https://doi.org/10.1016/j.toxlet.2016.06.018.
16. Soriano-Ursúa, M. A., Farfán-García, E. D., López-Cabrera, Y., Querejeta, E., & Trujillo-Ferrara, J. G. (2014). Boron-containing acids: preliminary evaluation of acute toxicity and access to the brain determined by Raman scattering spectroscopy. *Neurotoxicology*, *40*, 8–15. https://doi.org/10.1016/j.neuro.2013.10.005.
17. Jensen J. P. (2006). The rise and fall of borax as an antiepileptic drug. *Archives of neurology*, *63*(4), 621–622. https://doi.org/10.1001/archneur.63.4.621.
18. Barrón-González, M., Montes-Aparicio, A. V., Cuevas-Galindo, M. E., Orozco-Suárez, S., Barrientos, R., Alatorre, A., Querejeta, E., Trujillo-Ferrara, J. G., Farfán-García, E. D., & Soriano-Ursúa, M. A. (2023). Boron-containing compounds on neurons: Actions and potential applications for treating neurodegenerative diseases. *Journal of inorganic biochemistry*, *238*, 112027. https://doi.org/10.1016/j.jinorgbio.2022.112027.
19. Cordova-Chávez, R. I., Carrasco-Ruiz, M. F., Rodríguez-Vera, D., Pérez-Capistrán, T., Tamay-Cach, F., Score, I. R., Abad-García, A. & Soriano-Ursúa, M. A. (2023). Boron-Containing Compounds for Prevention, Diagnosis, and Treatment of Human Metabolic Disorders. *Biological trace element research*, *201*(5), 2222–2239. https://doi.org/10.1007/s12011-022-03346-9.
20. Bruker. SAINT v8.37A, Bruker AXS Inc, Madison, WI, USA, 2015.
21. R.H. Blessing, An empirical correction for absorption anisotropy, *Acta Crystallogr*. A51 (1995) 33–38, https://doi.org/10.1107/S0108767394005726.
22. G.M. Sheldrick, A short history of SHELX, *Acta Crystallogr*. A64 (2008) 112–122, https://doi.org/10.1107/S0108767307043930.
23. L.J. Farrugia, WinGX and ORTEP for windows: an update, *J. Appl. Crystallogr*. 45 (2012) 849–854, https://doi.org/10.1107/S0021889812029111.
24. A.L. Spek, Structure validation in chemical crystallography, *Acta Crystallogr*. D65 (2009) 148–155, https://doi.org/10.1107/S090744490804362X.
25. C.F. Macrae, I.J. Bruno, J.A. Chisholm, P.R. Edgington, P. McCabe, E. Pidcock, L. Rodriguez-Monge, R. Taylor, J. van de Streek, P.A. Wood, Mercury–CSD, New features for the visualization and investigation of crystal structures, *J. Appl. Crystallogr*. 41 (2008) 466–470, https://doi.org/10.1107/S0021889807067908.
26. Arulanandam, C.D., Hwang, JS., Rathinam, A.J. *et al.* Evaluating different web applications to assess the toxicity of plasticizers. *Sci Rep* 12, 19684 (2022). https://doi.org/10.1038/s41598-022-18327-0
27. Daina, A., Michielin, O. & Zoete, V. SwissADME: a free web tool to evaluate pharmacokinetics, drug-likeness and medicinal chemistry friendliness of small molecules. *Sci Rep* 7, 42717 (2017). https://doi.org/10.1038/srep42717.

28. Gfeller, D., Grosdidier, A., Wirth, M., Daina, A., Michielin, O., & Zoete, V. (2014). SwissTargetPrediction: a web server for target prediction of bioactive small molecules. *Nucleic acids research*, *42*(Web Server issue), W32–W38. https://doi.org/10.1093/nar/gku293.
29. Jarrahpour A., Motamedifar M., Zarei M., Youssoufi M.H., Mimouni M., Chohan Z.H., Ben Hadda T. (2010). Petra, Osiris, and molinspiration together as a guide in drug design: predictions and correlation structure/antibacterial activity relationships of new N-sulfonyl monocyclic β-lactams, phosphorus. Sulfur. *Silicon Relat. Elem*, 185:491–497. https://doi.org/10.1080/10426500902953953.
30. Lin, X., Li, X., & Lin, X. (2020). A Review on Applications of Computational Methods in Drug Screening and Design. *Molecules (Basel, Switzerland)*, *25*(6), 1375. https://doi.org/10.3390/molecules25061375.
31. Sliwoski, G., Kothiwale, S., Meiler, J., & Lowe, E. W., Jr (2013). Computational methods in drug discovery. *Pharmacological reviews*, *66*(1), 334–395. https://doi.org/10.1124/pr.112.007336.
32. Lorke D. (1983). A new approach to practical acute toxicity testing. *Archives of toxicology*, *54*(4), 275–287. https://doi.org/10.1007/BF01234480.
33. Bin, C., Xiaohui, W., Mengrou, S., Xin, L., Ting, Z., & Ping, G. (2021). Preliminary evaluation of the efficacy and safety of brimonidine for general anesthesia. *BMC anesthesiology*, *21*(1), 305. https://doi.org/10.1186/s12871-021-01516-1.
34. Prut, L., & Belzung, C. (2003). The open field as a paradigm to measure the effects of drugs on anxiety-like behaviors: a review. *European journal of pharmacology*, *463*(1-3), 3–33. https://doi.org/10.1016/s0014-2999(03)01272-x.
35. Gallop, P. M., Paz, M. A., & Henson, E. (1982). Boradeption: a new procedure for transferring water-insoluble agents across cell membranes. *Science (New York, N.Y.)*, *217*(4555), 166–169. https://doi.org/10.1126/science.6178158.
36. Altamore, T. M., Duggan, P. J., & Krippner, G. Y. (2006). Improving the membrane permeability of sialic acid derivatives. *Bioorganic & medicinal chemistry*, *14*(4), 1126–1133. https://doi.org/10.1016/j.bmc.2005.09.028.
37. Duggan, P., Houston, T., Kiefel-Levonis, S, Smith-Szydzik, M. L. (2008) Enhanced Fructose, Glucose and Lactose Transport Promoted by a 2-(Aminomethyl) phenylboronic Acid. *Tetrahedron*. 6471227126. https://doi.org/10.1016/j.tet.2008.05.052.
38. Coxon B. (2009). Developments in the Karplus equation as they relate to the NMR coupling constants of carbohydrates. *Advances in carbohydrate chemistry and biochemistry*, *62*, 17–82. https://doi.org/10.1016/S0065-2318(09)00003-1.
39. Williams, D. H. & Bhacca, N. S. (1964). Dependency of Vicinal Coupling Constants on the Configuration of Electronegative Substituents. *Journal of the American Chemical Society*, 86(13), 2742–2743. https://doi.org/10.1021/ja01067a060.
40. Ramsay, W. J., & Bayley, H. (2018). Single-Molecule Determination of the Isomers of d-Glucose and d-Fructose that Bind to Boronic Acids. *Angewandte Chemie (International ed. in English)*, *57*(11), 2841–2845. https://doi.org/10.1002/anie.201712740.
41. Lorand, J. P.; Edwards, J. O. (1959). Polyol Complexes and Structure of the Benzeneboronate Ion. *The Journal of Organic Chemistry*, 24(6), 769–774. https://doi.org/10.1021/jo01088a011.
42. Nishiyabu, R., Kubo, Y., James, T. D., & Fossey, J. S. (2011). Boronic acid building blocks: tools for sensing and separation. *Chemical Communications*, 47(4), 1106-1123. https://doi.org/10.1039/c0cc02920c.
43. Larkin, J. D., Fossey, J. S., James, T. D., Brooks, B. R., & Bock, C. W. (2010). A computational investigation of the nitrogen-boron interaction in o-(N,N-dialkylaminomethyl)arylboronate systems. *The journal of physical chemistry*. A, 114(47), 12531–12539. https://doi.org/10.1021/jp1087674.
44. Bull, S. D., Davidson, M. G., van den Elsen, J. M., Fossey, J. S., Jenkins, A. T., Jiang, Y. B., Kubo, Y., Marken, F., Sakurai, K., Zhao, J., & James, T. D. (2013). Exploiting the reversible covalent bonding of boronic acids: recognition, sensing, and assembly. *Accounts of chemical research*, 46(2), 312–326. https://doi.org/10.1021/ar300130w.
45. Suzuki, Y., Shimizu, M., Okamoto, T., Sugaya, T., Iwatsuki, S., Inamo, M., Takagi, H. D., Odani, A. & Ishihara, K. (2016). Detailed Mechanism of the Reaction of Phenylboronic Acid Derivatives with D-Fructose in Aqueous Solution: A Comprehensive Kinetic Study. *ChemistrySelect*. 1: 5141-5151. https://doi.org/10.1002/slct.201600875.
46. Nunez, H. A., Walker, T. E., Fuentes, R., O'Connor, J., Serianni, A., & Barker, R. (1977). Carbon-13 as a tool for the study of carbohydrate structures, conformations and interactions. *Journal of supramolecular structure*, *6*(4), 535–550. https://doi.org/10.1002/jss.400060407.
47. Nobre, C., Teixeira, J. A., & Rodrigues, L. R. (2015). New Trends and Technological Challenges in the Industrial Production and Purification of Fructo-oligosaccharides. *Critical reviews in food science and nutrition*, *55*(10), 1444–1455. https://doi.org/10.1080/10408398.2012.697082.
48. Rodrigues-Borges, M. & de Carvalho-Balaban, R. (2014). L-Arabinose (pyranose and furanose rings)-branched poly(vinyl alcohol): Enzymatic synthesis of the sugar esters followed by free radical polymerization. Journal of Biotechnology, 192: 42-49. https://doi.org/10.1016/j.jbiotec.2014.10.005.

 doi:10.20944/preprints202405.1343.v1

49. .Dimmitt, S., Stampfer, H., & Martin, J. H. (2017). When less is more - efficacy with less toxicity at the ED50. *British journal of clinical pharmacology*, *83*(7), 1365–1368. https://doi.org/10.1111/bcp.13281.
50. Varughese, S., Azim, Y., & Desiraju, G. R. (2010). Molecular complexes of alprazolam with carboxylic acids, boric acid, boronic acids, and phenols. Evaluation of supramolecular heterosynthons mediated by a triazole ring. *Journal of pharmaceutical sciences*, *99*(9), 3743–3753. https://doi.org/10.1002/jps.22117.
51. Goldschen-Ohm M. P. (2022). Benzodiazepine Modulation of GABAA Receptors: A Mechanistic Perspective. *Biomolecules*, *12*(12), 1784. https://doi.org/10.3390/biom12121784.
52. Wisniak, J. (2005). Borax, Boric Acid and Boron-From Exotic to Commodity. *Indian Journal of Chemical Technology*, 12: 488-500.
53. Grand, R.S. & Wegner, E.S. (1948). Fatal case of boric acid poisoning. *Am J Dis Child*, 6: 910-912.
54. Bean, E.O. (1949). Accidental ingestion of boric acid. *Clin Proc Child Hosp Dist Columbia*, 4: 101-103.
55. Restuccio, A., Mortensen, M. E., & Kelley, M. T. (1992). Fatal ingestion of boric acid in an adult. *The American journal of emergency medicine*, *10*(6), 545–547. https://doi.org/10.1016/0735-6757(92)90180-6.
56. Hamilton, R. A., & Wolf, B. C. (2007). Accidental boric acid poisoning following the ingestion of household pesticide. *Journal of forensic sciences*, *52*(3), 706–708. https://doi.org/10.1111/j.1556-4029.2007.00420.x.
57. Duydu, Y., Basaran, N. & Hermann, B.M. (2015). Human health risk assessment of boric acid and sodium borates. *Toxicol Lett*, 238: S102-103. https://doi.org/10.1016/j.toxlet.2015.08.338.
58. White, H. S., Brown, S. D., Woodhead, J. H., Skeen, G. A., & Wolf, H. H. (2000). Topiramate modulates GABA-evoked currents in murine cortical neurons by a nonbenzodiazepine mechanism. *Epilepsia*, *41*(S1), 17–20. https://doi.org/10.1111/j.1528-1157.2000.tb02165.x.
59. Shank, R. P., Gardocki, J. F., Streeter, A. J., & Maryanoff, B. E. (2000). An overview of the preclinical aspects of topiramate: pharmacology, pharmacokinetics, and mechanism of action. *Epilepsia*, *41*(S1), 3–9. https://doi.org/10.1111/j.1528-1157.2000.tb02163.x.
60. Mula, M., Cavanna, A. E., & Monaco, F. (2006). Psychopharmacology of topiramate: from epilepsy to bipolar disorder. *Neuropsychiatric disease and treatment*, *2*(4), 475–488. https://doi.org/10.2147/nedt.2006.2.4.475.
61. Zhang, X., Velumian, A. A., Jones, O. T., & Carlen, P. L. (2000). Modulation of high-voltage-activated calcium channels in dentate granule cells by topiramate. *Epilepsia*, *41*(S1), 52–60. https://doi.org/10.1111/j.1528-1157.2000.tb02173.x.
62. Dodgson, S. J., Shank, R. P., & Maryanoff, B. E. (2000). Topiramate as an inhibitor of carbonic anhydrase isoenzymes. *Epilepsia*, *41*(S1), 35–39. https://doi.org/10.1111/j.1528-1157.2000.tb06047.x.
63. Gibbs, J. W., 3rd, Sombati, S., DeLorenzo, R. J., & Coulter, D. A. (2000). Cellular actions of topiramate: blockade of kainate-evoked inward currents in cultured hippocampal neurons. *Epilepsia*, *41*(S1), 10–16. https://doi.org/10.1111/j.1528-1157.2000.tb02164.x.